

Molecular topology in ethylene copolymers studied by means of mechanical testing

R. SEGUELA, F. RIETSCH

Laboratoire de Structure et Propriétés de l'Etat Solide, LA 234, Université des Sciences et Techniques de Lille Flandres Artois, 59655 Villeneuve d'Ascq Cédex, France

The molecular topology of melt-crystallized ethylene-1-butene copolymers has been investigated by means of mechanical testing with the aid of suitable models. The number of regular folds between two consecutive interlamellar tie molecules has been estimated by means of a theoretical relationship of the tensile modulus as a function of temperature. In addition, the molecular weight between entanglements of the copolymers has been determined from an analysis of the post-yield strain-hardening, assuming an ideal network behaviour. It has been shown that the regular folded chain macroconformation turns gradually into a fringed micellar macroconformation as the co-unit concentration increases. The entanglement density increases in parallel. These results confirm the conclusion of a previous work stating that the rejection of the co-units within the amorphous phase disturbs the basic chain folding mechanism of crystallization and hampers the "reeling-in" motion of the chains from the melt on to the growth surfaces. Criticisms of the models have been developed taking into account some inconsistent aspects with regard to the experimental data.

1. Introduction

Since the discovery of the chain-folded structure of polymer crystals, the topological characterization of the crystal surface constituted by the chain folds has been a matter of deep controversy [1]. Some authors claim that the chains fold back regularly with predominant adjacent re-entry, while other authors argue for a disordered surface made up of irregular folds having random re-entry. An additional point of dispute connected with the mechanism of regular folding has occurred about the existence of the "reeling-in" motion of the chains and the accompanying disentanglement effect during the course of crystallization.

Nevertheless, it has been pointed out by Wunderlich [2] and Mandelkern [3] that defects in the molecular structure such as co-units, branches or stereoirregularities are liable to increase the disorder in the crystal surface. We have already assented to this hypothesis in a study dealing with the drawing behaviour of ethylene-1-butene copolymers [4]. Indeed, we have shown that the co-unit concentration controls the strain-hardening effect together with the maximum achievable draw ratio. This phenomenon has been interpreted in terms of topological modifications of the molecular network related to the pseudo-eutectic nature of ethylene-1-butene copolymers, i.e. the propensity for rejection of the co-units within the amorphous phase which disturbs the regular chain folding and increases the disorder in the crystal surface.

We report here an endeavour at quantitative investigation of the chain topology in the copolymers previously studied, by means of mechanical testing. The basis of this approach relies on the generally

admitted proposal that the chain topology has an overriding effect on the mechanical properties [3, 5]. From tensile modulus measurements as a function of temperature, we have been able to characterize the chain-folded structure of the amorphous intercrystalline layer thanks to the model of Krigbaum *et al.* [6] which involves a molecular parameter in the theoretical treatment of the modulus of semi-crystalline polymers. The parameter in question is defined as the chain length between two consecutive nucleation sites from which crystallization proceeds by chain folding. On the other hand, the approach of Mills *et al.* [7] for the post-yield behaviour of semi-crystalline polymers provided us with a means to evaluate the molecular weight between entanglements of the copolymers. The basic assumption of this over-simplified model is that the strain-hardening which takes place after necking results mainly from the extension of a molecular network and can be thus treated in the framework of rubber elasticity theory.

2. Materials and experimental methods

The polymers studied are ethylene-1-butene copolymers having very similar molecular weights and containing various concentrations of 1-butene co-units. The molecular and physical characteristics of the copolymers are listed in Table I (see Seguela and Rietsch [4] for more details).

The polymers were compression-moulded into sheets at 190°C and allowed to relax in the press in the molten state for a period of 10 min before cooling at about 50°C min⁻¹.

Density and calorimetric data were obtained according to the procedures described elsewhere [8].

TABLE I Molecular and physical characteristics of the polymers studied

Sample	$\bar{M}_w \times 10^{-3}$	$\bar{M}_n \times 10^{-3}$	Co-unit content (mol %)	Density (g cm ⁻³)	Crystal weight-fraction from differential scanning calorimetry
PE-1	135	15	Virtually nil	0.960	0.73
PE-2	157	30	0.6	0.950	0.66
PE-3	178	19	1.1	0.943	0.62
PE-4	136	31	2.5	0.930	0.53
PE-5	140	29	5	0.919	0.43

Dynamic mechanical measurements were carried out on a Toyo Baldwin Rheovibron DDVIB operated at a frequency of 3.5 Hz. The samples tested were about 2.5 mm wide, 0.25 mm thick and 40 mm in gauge length. The temperature range [−50 to +140°C] was scanned at a heating rate of about 1°C min⁻¹. Corrections of the experimental data allow for the apparatus compliance and sample shearing within the grips were performed as a function of temperature, according to the method of the infinitely short sample suggested by the apparatus manufacturer [9].

Drawing experiments were carried out at a cross-head speed of 50 mm min⁻¹ in an Instron tensile testing machine provided with an environmental chamber. Dumbbell-shaped samples with 16 mm and 4 mm gauge length and width, respectively, were cut out from sheets about 1.7 mm thick.

A small-angle X-ray scattering (SAXS) study was performed in the photographic mode, using a Luzati-Baro camera equipped with two pinhole collimators 0.5 and 0.3 mm in diameter. The second collimator, the sample and the film were placed at 360, 370 and 780 mm from the first collimator, respectively. The CuK α radiation was filtered with nickel foil from the emission of a Siemens X-ray tube operated at 40 kV and 20 mA. Exposure times of 24 h were used for 0.25 mm thick samples.

3. Results and discussion

3.1. Chain macroconformation related to the crystallization

The theoretical treatment of the tensile modulus of semi-crystalline polymers developed by Krigbaum *et al.* [6] can be used for studying the chain folding structure since it involves a molecular parameter directly connected with the crystallization mechanism. Fig. 1 depicts the crystallization of a chain portion after deposition of the chain on to the growth surfaces of two lamellar crystals. The basic parameter N of the model is defined as the contour length of the chain portion between the two nucleation sites, expressed as a number of statistical segments. Each nucleation event gives rise to an intercrystalline tie-chain while the chain portion between the points of initial anchoring is assumed to undergo a chain-folded crystallization.

The mechanical model is based on the assumption that most of the deformation is accommodated within the amorphous phase, the crystallites acting only as physical crosslinks. In addition, the specific behaviour of the amorphous phase is analysed in the framework of the Langevin statistical treatment of rubber elasticity, since the crystallization advancement is expected

to bring the mechanically active tie-chains to a highly strained state which is characterized by the parameter β according to the relation

$$\beta = \mathcal{L}^{-1}[1/N^{1/2}(1 - \alpha)] \quad (1)$$

where α is the crystal weight-fraction in the sample.

The parameter β can also be derived from thermodynamic considerations, leading to the following temperature dependency [10]:

$$\frac{\sinh \beta}{\beta} = \exp \left[\frac{\Delta H_f}{R} \left(\frac{1}{T} - \frac{1}{T_m^0} \right) \right] \quad (2)$$

where T_m^0 is the final melting temperature of the polymer and ΔH_f the melting enthalpy per mole of statistical segment.

In this context, the tensile modulus is given by

$$E = \frac{\rho RT}{M_0} \times \left(\frac{\beta^2 \sinh^2 \beta}{5N(1 - \alpha)^3(\sinh^2 \beta - \beta^2)} + \frac{4\beta}{5N^{1/2}(1 - \alpha)} \right) \quad (3)$$

where ρ is the density of the polymer and M_0 the molecular weight of the statistical segment [6].

Taking into account that the statistical segment for polyethylene is composed of ten methylene units [11, 12], the following physical constants can be adopted for the calculations concerning homopolyethylenes and pseudo-eutectic copolymers:

$$T_m^0 = 140^\circ \text{C} \quad M_0 = 140 \text{ g mol}^{-1} \\ \Delta H_f = 40 \text{ kJ mol}^{-1}$$

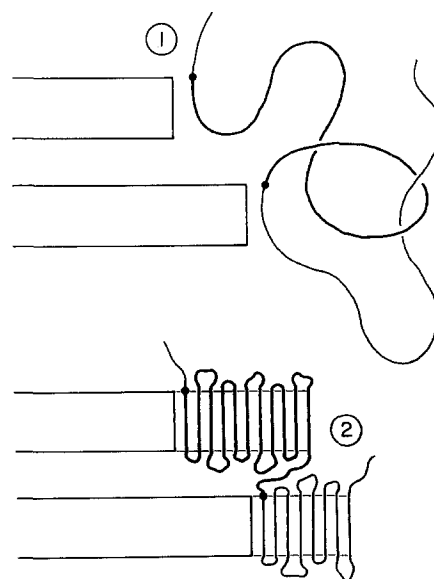


Figure 1 Mechanism of chain folding according to the Krigbaum model: (1) nucleation step, (2) growth step (see text for details).

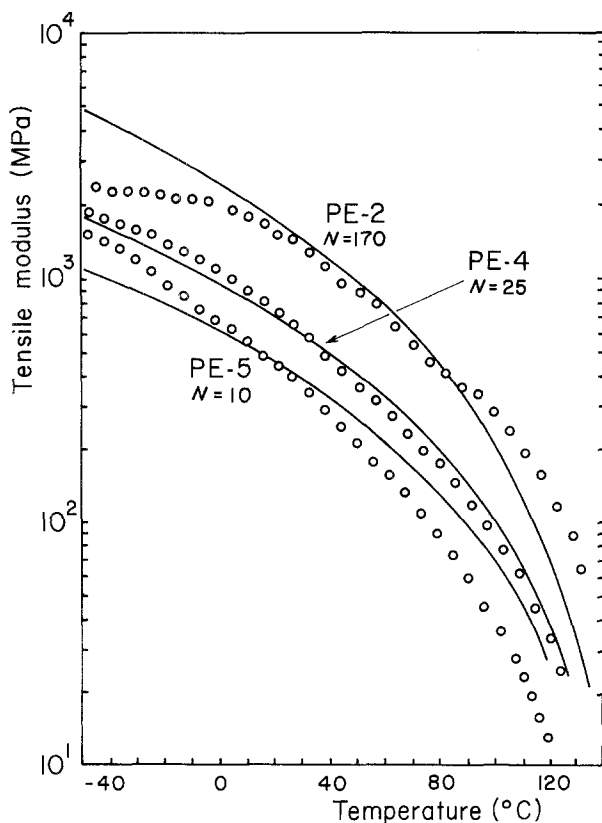


Figure 2 Tensile modulus of polymers PE-2, PE-4 and PE-5 as a function of temperature: (O) experimental data, (—) theoretical curves from Equation 3.

In addition, the density dependence on the crystal weight-fraction is given by the relation

$$\alpha = \frac{\rho_c}{\rho} \left(\frac{\rho - \rho_a}{\rho_c - \rho_a} \right) \quad (4)$$

assuming a perfect two-phase model with the values $\rho_a = 0.855 \text{ g cm}^{-3}$ and $\rho_c = 1.00 \text{ g cm}^{-3}$ for the amorphous and crystal densities, respectively, in the case of polyethylene [8].

Henceforth, by computing the crystallinity from Equation 1 after calculation of the parameter β according to Equation 2, the theoretical curve for the tensile modulus as a function of temperature can be determined from Equation 3, using a successive adjustment procedure of N for best fitting with the experimental data. Fig. 2 shows the tensile modulus data obtained as a function of temperature for the polymers PE-2, PE-4 and PE-5 (Table I), together with the best fitted theoretical curves. The data concerning the polymers PE-1 and PE-3 are not shown for the sake of clarity.

The values of the parameter N obtained for the five samples studied are reported in Table II. Also given in

Table II are the values of the SAXS long period d together with the crystal thickness d_c determined from the equation

$$d_c = \frac{\rho}{\rho_c} \alpha d \quad (5)$$

The number of statistical segments N_c in a crystalline stem assumed to be normal to the crystal surface is given by

$$N_c = \frac{d_c}{10(c/2)} \quad (6)$$

where $c = 0.255 \text{ nm}$ is the unit cell parameter along the chain axis for polyethylene. The average number of crystalline stems \bar{n} interconnected in a regular folding fashion can be estimated from the ratio

$$\bar{n} = \alpha N / N_c \quad (7)$$

The values of \bar{n} reported in Table II exhibit a drastic drop that reveals a strong topological change from a regular chain-folded macroconformation to a fringed micellar macroconformation as the crystallinity decreases from PE-1 to PE-5. In other words, $\bar{n} = 16$ for PE-1 is relevant to Regime I or II of crystal growth after Hoffmann [13], both regimes involving few nucleation events compared with the incidence of regular folding. On the other hand, $\bar{n} \simeq 1$ for PE-5 reveals the occurrence of a nucleation event after almost every stage of crystalline stem deposition according to Regime III of crystal growth [14]. This is in perfect agreement with our previous interpretation of the co-unit effect on the molecular topology of ethylene-1-butene copolymers, i.e. the disturbance of the chain folding process as a result of co-unit segregation within the amorphous phase [4].

Schematic representations of three different topological situations are given in Fig. 3. It is worth mentioning that, according to the calculations above, the n -times regular folding of a chain between two intercrystalline tie-molecules does not necessarily imply a strictly adjacent mode of chain re-entry. It just means that the folds are tight enough (i.e. close neighbour re-entry) to avoid intertwinning of loops from opposite crystalline lamellae. As a matter of fact, two interlocked loops from neighbouring lamellae are likely to behave as two tie-chains (see Fig. 3b), even though such a topological defect should not obligatorily be related to a nucleation event as postulated in the Krigbaum model. The predominance of adjacent re-entry folding which characterizes Regime I of crystal growth can only be expected for highly linear homopolyethylene, in the case of dilute-solution crystallization or melt crystallization at very low undercooling.

TABLE II Structural and topological characteristics derived from tensile modulus and SAXS data

Samples	Krigbaum's parameter, N	SAXS long period, d (nm)	Crystal thickness, d_c (nm)	Crystalline stem length, N_c	Number of regular folds, \bar{n}
PE-1	350	29.5	20.5	16	16
PE-2	170	28.0	17.5	14	8
PE-3	110	24.5	14.5	11	6
PE-4	25	23.0	11.5	9	1.5
PE-5	10	22.0	8.5	6	1

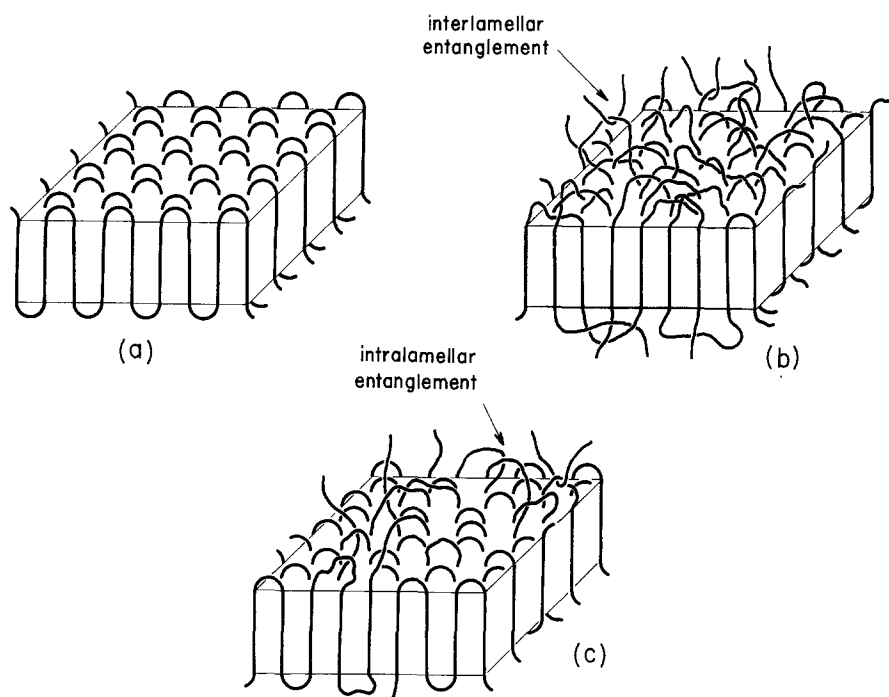


Figure 3 Different types of topological landscape in linear homopolyethylene and ethylene copolymers: (a) chain-folded macroconformation with adjacent re-entry, (b) fringed micellar macroconformation with random re-entry, (c) intermediate mixed macroconformation.

3.2. Entanglement density of the overall macromolecular network

Several authors [7, 15–17] have proposed different theoretical treatments of the post-yield behaviour of semi-crystalline polymers, considering separately the plastic deformation of the crystalline phase and the stretching of the macromolecular network which embraces both the crystal and the amorphous phase.

We have paid particular attention to the model of Mills *et al.* [7] which allows a direct determination of the molecular weight between entanglements, M_e , the entanglement points being defined as the physical chain crosslinks according to Fig. 3. This model assumes, as a first approximation, that plastic deformation of the crystalline phase is achieved under constant stress so that the post-yield strain-hardening effect can be roughly described by the stress-strain equation characteristic of a rubber network [18]:

$$\sigma_T = \frac{\rho RT}{M_e} (\lambda^2 - \lambda^{-1}) \quad (8)$$

where σ_T is the true stress and λ the draw ratio.

Mills *et al.* have reported that, in the case of linear and branched low-density polyethylenes, the variation curves of the true stress as a function of the Gaussian parameter ($\lambda^2 - \lambda^{-1}$) exhibited a fair linearity which lends credence to the model. In addition, the values of the molecular weight between entanglements deduced from the experimental data were quite realistic.

Starting from their successful experience, we have applied a similar analysis to our ethylene copolymers. However, our experiments have been conducted at the drawing temperature $T_d = 80^\circ\text{C}$, i.e. well above the α_c relaxation, in order that the crystals should be sufficiently ductile. Fig. 4 shows plots of the true stress as a function of the Gaussian parameter for the samples PE-1, PE-2 and PE-4. The data for PE-3 and PE-5 are not shown in order to avoid a confused superposition of the results at low strains. The curves of Fig. 4 are fairly linear in a good part or over the full scale of the

investigated draw ratios. The slopes of the straight parts of the curves are reported in Table III for the five polymers studied, together with the crystal weight-fractions of the samples at the drawing temperature $T_d = 80^\circ\text{C}$ estimated from differential scanning calorimetry (DSC) measurements, and the corresponding densities computed from Equation 4. The values of M_e shown in the last column of Table III decrease markedly with crystallinity. This behaviour corroborates our previous conclusion [4] concerning the adverse influence of the non-crystallizable co-units on the reeling-in motion of the chains and the concomitant disentanglement during the course of crystallization.

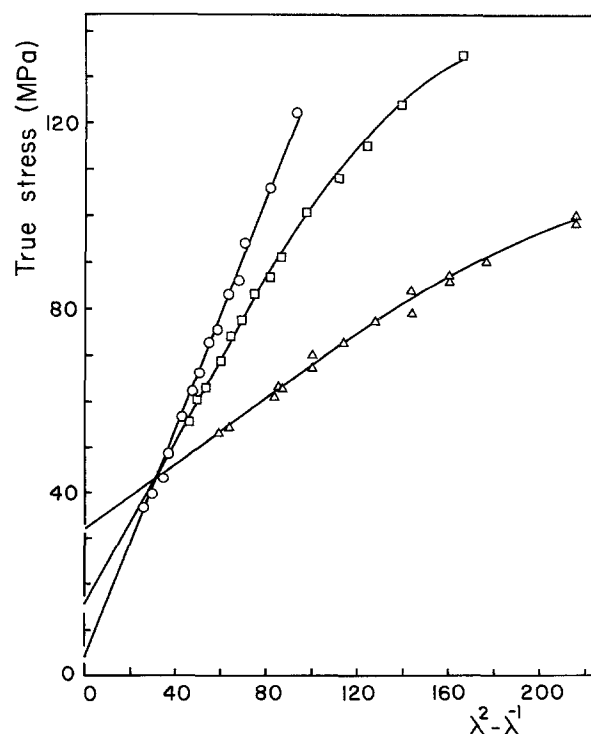


Figure 4 True stress in the strain-hardening range for polymers (Δ) PE-1, (\square) PE-2 and (\circ) PE-4 as a function of the Gaussian parameter.

TABLE III Physical data for strain hardening at 80°C

Samples	α^{80°	ρ^{80° (g cm ⁻³)	$\rho RT/M_c$ (MPa)	M_c (g mol ⁻¹)
PE-1	0.73	0.958	0.36	7800
PE-2	0.66	0.944	0.89	3100
PE-3	0.62	0.940	1.07	2600
PE-4	0.46	0.916	1.24	2200
PE-5	0.32	0.897	1.10	2400

However, a very striking feature of Table III is that the molecular weight between entanglements levels off about a value $M_c \approx 2200$ g mol⁻¹ which is astonishingly close to the average value $M_c \approx 2000$ g mol⁻¹ reported for molten polyethylene [19–21], according to the determination of the critical molecular weight from viscosity measurements. This result gives a clear indication that for a co-unit concentration greater than about 1% (see Table I), the chain folding process is so much disturbed that the reeling-in motion of the chains is quite frozen and the entanglement density characteristic of the molten state is preserved throughout the crystallization.

It must be noticed that, except for copolymers PE-5, the values of M_c are lower than the molecular weight of the chains between the anchoring points calculated from the values of N . This suggests that most of the entanglements remaining after crystallization do not give rise to intercrystalline links, in other words the entanglements are more likely to be intralamellar rather than interlamellar (see Figs 3b and c). A reason for this lies in the fact that two entangled chains crystallizing on the growth surfaces of two different crystallites should be more prone to disentangle than two chains which crystallize close together in the same lamella. In this connection, most of the entanglements cannot contribute to the low-strain deformation but become active in drawing at large strains owing to the fragmentation of the crystalline lamellae into blocks which takes place during the necking process.

4. Critical remarks about the models

4.1. The Krigbaum model

The application of Krigbaum's approach involves a fitting procedure according to which the molecular parameter N is successively adjusted to achieve best agreement between the theoretical temperature-dependent variation of the tensile modulus and the experimental data. The use of the experimentally determined values of the crystallinity of our samples for the computation of Equation 3 led to unreasonably low values of N for the copolymers PE-4 and PE-5, namely N was much smaller than the number N_c of statistical segments in a single crystalline stem estimated from SAXS according to Equations 5 and 6. Crystallinity values were therefore calculated from the theoretically derived Equation 1 which gives much higher values than the experimental ones, N being the same as for the calculation of the tensile modulus from Equation 3. For the sake of comparison, Figs 5 and 6 show the temperature dependence of the experimental and theoretically predicted crystal weight fractions, respectively, for the case of copolymers PE-2, PE-4 and PE-5.

The higher value of the theoretical crystallinity can

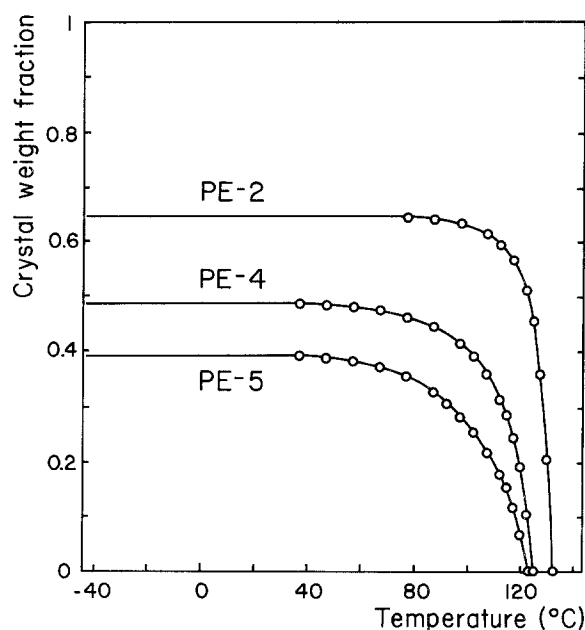


Figure 5 DSC crystallinity data for polymers PE-2, PE-4 and PE-5 as a function of temperature.

in fact be considered as an “equivalent crystallinity” for the pure *series* model of phase association which supports Krigbaum's model, through the assumption that the deformation is almost entirely borne by the amorphous phase. As a matter of fact, there is no doubt that the spherulitic structure of polyethylene could be regarded as a series model for most of the deformation modes induced by low strains, owing to the isotropic treatment of the amorphous phase. Fig. 7 depicts several types of motion of the lamellar ribbons which should effectively involve an elastically reversible deformation of the intercrystalline amorphous phase, in a spherulitic structure submitted to a uniaxial stretch. However, it is perfectly clear from Fig. 7 that the crystalline ribbons parallel to the tensile direction undergo an elongation for which a series model is

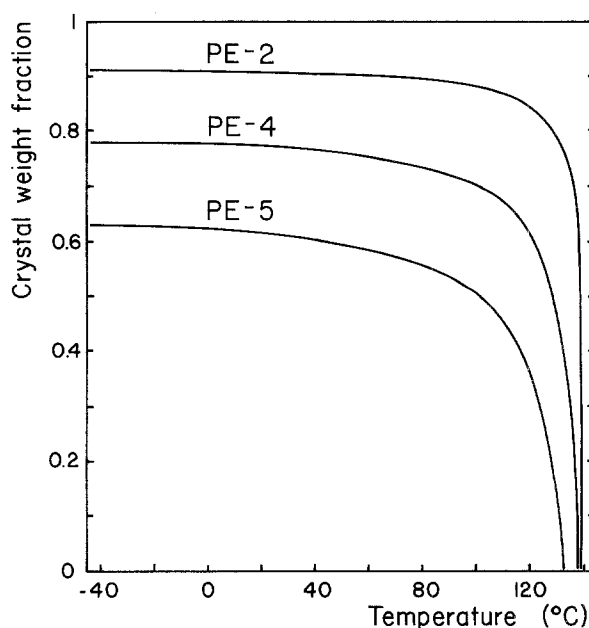


Figure 6 Predicted crystallinity for polymers PE-2, PE-4 and PE-5 as a function of temperature, according to Equation 1 (N is the same as for the calculations of the storage modulus presented in Fig. 2).

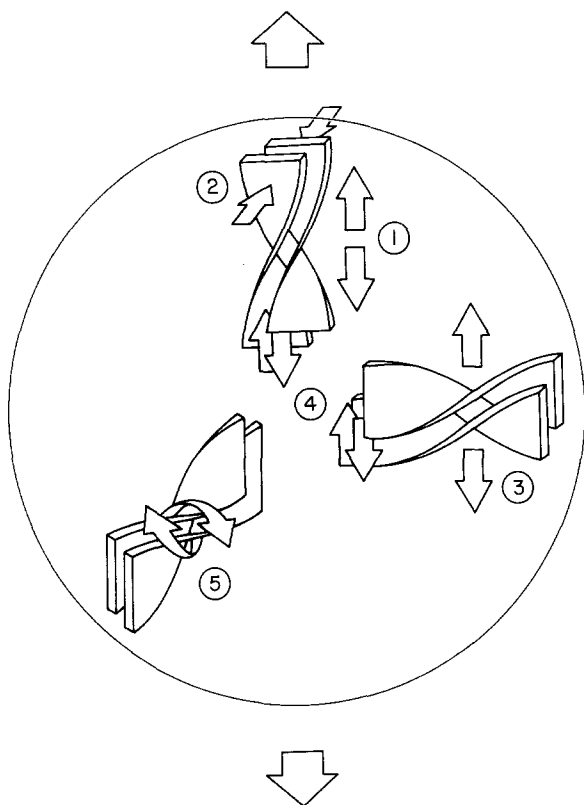
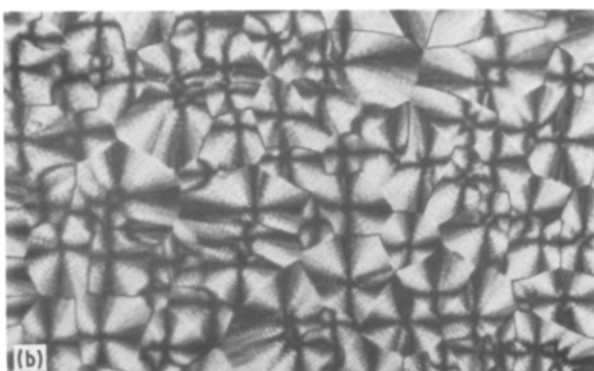


Figure 7 Schematic representation of local deformation modes in a spherulitic structure submitted to a uniaxial elastic stretch: (1) lamellar elongation, (2) transverse lamellar compression, (3) lamellar separation, (4) lamellar slip, (5) lamellar rotation.

absolutely untenable. Thus, the use of the overestimated theoretical values of the crystallinity for the calculation of the tensile modulus as a function of temperature affords a means of taking into account the small part of *parallel* character of the spherulitic structure which is not considered in the Krigbaum model.

The discussion above applies perfectly to the copoly-



mers investigated in this work owing to the fact that the crystallization conditions used for the preparation of the mechanical test pieces give rise to well-defined spherulitic structures, as revealed on the optical micrographs of Fig. 8. It is yet to be noted that, as the crystallinity decreases, the superstructure decays gradually from the large ringed spherulites impinging on each other to the small coarse-featured spherulites barely connected to one another.

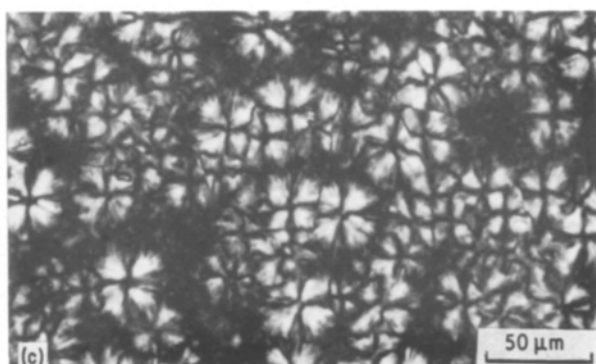
To finish with, it is well known that semi-crystalline polymers exhibit a molecular α_c relaxation within the crystal which involves a decay of the elastic modulus with increasing temperature, independently of the decrease of crystallinity. The fact that the Krigbaum model does not take this effect into consideration may be an explanation for the discrepancies that can be observed in Fig. 2 between the experimental and predicted variations of the modulus. Therefore, one must pay much more attention to the drastic change of the parameter N as a function of the co-unit concentration in the polymers than to the values of N themselves.

4.2. The Haward model

In view of the very small change in the crystallite size distribution, Mills *et al.* [7] have concluded that the deformation of low-density polyethylene beyond necking at ambient temperature relies on the extension of the amorphous regions alone. Consequently, these authors have considered that the molecular weight between entanglements deduced from their analysis refers to the amorphous phase.

We do not share this standpoint since the post-yield behaviour of polyethylene is basically plastic and cannot be assigned solely to the deformation of the rubbery amorphous phase. It has indeed been largely shown that the crystalline phase does take part in the deformation process at large strains, notably through chain unfolding [22–24]. Moreover, the prime role of the macromolecular network embracing both the crystalline and amorphous phases has been clearly pointed out from the shrinkage behaviour of polyethylene fibres upon heating in the melting-temperature range [17, 25]. So, although chain entanglements should be liable to gather in the amorphous phase, the molecular weight between entanglements determined from the

Figure 8 Optical micrographs of polymers (a) PE-1, (b) PE-3 and (c) PE-5 between crossed polarizers.



analysis of the strain-hardening behaviour must be related to the overall molecular network.

As a corollary to the proposition of Mills *et al.* [7], independently of the preceding criticism, the ultimate draw ratio of any polyethylene could be roughly predicted from the value of the molecular weight between entanglement, M_e , according to the commonly used relation

$$\lambda_{\max} = n_e^{1/2} \quad (9)$$

derived from the extension limit of a single entangled chain, in which n_e is the number of statistical segments between entanglements. Remembering that the statistical segment of polyethylene consists of ten methylene units, one might expect the drawing limits $\lambda_{\max} = 7.5$ for PE-1 and $\lambda_{\max} = 4.0$ for PE-5. These values are far below the maximum draw ratios actually achievable by hot drawing [4]. In addition, the stress upswing that should occur as the draw ratio approaches the extension limit of the network, according to the well-known behaviour of crosslinked rubbers [18], has not been observed in our study, as well as in the work reported by Mills *et al.* [7]. This apparent contradiction between the model and the experimental data might arise from the contribution of some secondary phenomena taking place concurrently with the extension of the uncrosslinked network at large strains. For instance, slippage and disentanglement of some strained chains [25–27], crazing [28, 29] and microfibril sliding [24–30] are such processes that do not occur in conventional rubbers but do take part in the deformation of semi-crystalline polymers.

5. Conclusions

In spite of some deficient features, the two models used in this work provide a valuable means to characterize the topological behaviour of semi-crystalline polymers and allow us to draw interesting conclusions about the influence of chain structure irregularities on the crystallization mechanism of the chains from the melt.

The present investigation is particularly relevant to the occurrence of either chain-folded or fringed micellar macroconformations depending on the concentration of the 1-butene units in ethylene copolymers. It provides numerical estimates of the number of consecutive regular folds between two nucleation sites of the chains, together with the molecular weight between entanglements of the overall network of the copolymers, both of which support our previous work on the tensile drawing behaviour of these copolymers.

It is suggested that the rejection of the co-units within the amorphous phase breaks off the basic chain-folding mechanism of crystallization of the methylenic chains. This phenomenon is also likely

to impede the reeling-in of the chains on to the growth surface of the crystals during the course of crystallization, precluding thus the disentanglement of the coils from the melt.

References

1. *Faraday Discuss. Chem. Soc.* **68** (1979).
2. B. WUNDERLICH, "Macromolecular Physics", Vol. 3 (Academic, New York, 1980) pp. 262, 307.
3. L. MANDELKERN, *Polym. J.* **17** (1985) 337.
4. R. SEGUELA and F. RIETSCH, *Polymer* **27** (1986) 703.
5. G. CAPACCIO, T. A. CROMPTON and I. M. WARD, *J. Polym. Sci., Polym. Phys. Edn* **14** (1976) 1641.
6. W. R. KRIGBAUM, R.-J. ROE and K. J. SMITH JR, *Polymer* **5** (1964) 533.
7. P. J. MILLS, J. N. HAY and R. N. HAWARD, *J. Mater. Sci.* **20** (1985) 501.
8. R. SEGUELA and F. RIETSCH, *Polymer* **27** (1986) 532.
9. Instruction Manual for Direct Reading Dynamic Viscoelastometer Rheovibron Model DDVIIIB (Toyo Baldwin, Tokyo, 1969) p. 30.
10. R.-J. ROE, K. J. SMITH JR and W. R. KRIGBAUM, *J. Chem. Phys.* **35** (1961) 1306.
11. M. V. VOLKENSTEIN, "Configurational Statistics of Polymeric Chains" (Wiley-Interscience, New York, 1963) p. 429.
12. P. J. FLORY, "Statistical Mechanics of Chain Molecules" (Wiley-Interscience, New York, 1969) p. 12.
13. J. D. HOFFMAN, *Polymer* **23** (1982) 656.
14. *Idem, ibid.* **24** (1983) 3.
15. B. HEISE, H.-G. KILLIAN and W. WULFF, *Prog. Colloid Polym. Sci.* **67** (1980) 143.
16. S. ICHIHARA and S. IIDA, in "The Strength and Stiffness of Polymers", edited by A. E. Zachariades and R. S. Porter (Dekker, New York, 1983) Ch. 4.
17. I. M. WARD, *Polym. Engng Sci.* **24** (1984) 724.
18. L. R. G. TRELOAR, "The Physics of Rubber Elasticity" (Oxford University Press, London, 1967) pp. 64–122.
19. R. S. PORTER and J. F. JOHNSON, *Chem. Rev.* **66** (1966) 1.
20. D. W. Van KREVELEN, "Properties of Polymers" (Elsevier, Amsterdam, 1976) p. 339.
21. W. W. GRAESSELEY and S. F. EDWARDS, *Polymer* **22** (1981) 1329.
22. A. PETERLIN, *Colloid Polym. Sci.* **253** (1975) 809.
23. *Idem, J. Appl. Phys.* **48** (1977) 4099.
24. *Idem*, in "Ultra-High Modulus Polymers", edited by A. Ciferri and I. M. Ward (Applied Science, London, 1979) Ch. 10.
25. G. CAPACCIO and I. M. WARD, *Colloid Polym. Sci.* **260** (1982) 46.
26. P. SMITH, P. J. LEMSTRA and H. C. BOOIJ, *J. Polym. Sci., Polym. Phys. Edn* **19** (1981) 877.
27. D. T. GRUBB, *ibid.* **21** (1983) 165.
28. T. JUSKA and I. R. HARRISON, *Polym. Engng Sci.* **22** (1982) 766.
29. *Idem, Polym. Engng Rev.* **2** (1982) 13.
30. A. PETERLIN, *Int. J. Fract.* **11** (1975) 761.

Received 7 January
and accepted 15 May 1987